Heliyon 6 (2020) e04636

Contents lists available at ScienceDirect

Heliyon

journal homepage: www.cell.com/heliyon

Research article

Green synthesis and characterization of copper nanoparticles using *Piper retrofractum Vahl* extract as bioreductor and capping agent

Suci Amaliyah [a], Dwika Putri Pangesti [a], Masruri Masruri [a], Akhmad Sabarudin [a,*], Sutiman Bambang Sumitro [b]

[a] *Department of Chemistry, Faculty of Science, Brawijaya University, Malang 65145, Indonesia*
[b] *Departement of Biology, Faculty of Science, Brawijaya University, Malang 65145, Indonesia*

ARTICLE INFO

Keywords:
Materials science
Materials chemistry
Nanotechnology
Green synthesis
Piper retrofractum
Copper nanoparticles
Plant extract

ABSTRACT

The copper nanoparticles (CuNPs) have attracted much attention due to their application in diverse fields. The applications of CuNPs depend on their physical and chemical properties. This study presents the first report for the use of medicinal fruit extract of *Piper retrofractum Vahl* as an eco-friendly reagent in the synthesis of CuNPs using copper sulfate as a starting material. *Piper retrofractum Vahl* extract was employed as a bioreductor as well as a capping agent in the formation of CuNPs. The reaction process was assisted by sonication and stirring. The influences of extract concentration, pH, temperature, and reaction time on the size of CuNPs were studied in detail. The morphology and structure of synthesized CuNPs were characterized by UV-Vis, FT-IR, SEM-EDS, TEM, and XRD. The UV-Vis measurement showed the surface plasmon resonance (SPR) peak at 234-255 nm, whereas FTIR characteristic peaks of metal-oxygen (Cu–O) were confirmed in the range 550-570 cm^{-1} and Cu–O–H bonds led to bending absorptions in the region 870-880 cm^{-1}. The synthesized CuNPs possess the spherical shapes and high content of copper (70.3%) as confirmed by SEM-EDS. From the TEM micrograph, it can be seen that the particle size distribution of CuNPs has a high uniformity with a size of 2–10 nm under the optimum condition. The crystalline nature of CuNPs as confirmed by XRD showed the crystallinity phase of 26.4%. The synthesized CuNPs have relatively good stability and could inhibit *Escherichia coli* and *Staphylococcus aureus*. The results proved that *Piper retrofractum Vahl* fruit extract could be applied for a greener synthesis of CuNPs with high uniformity of particle sizes.

1. Introduction

Nanoparticles have attracted many researchers because of their unique properties compared to their bulk material [1, 2]. They have unique characteristics due to the size, shape, distribution, and morphology [1, 3]. One of the applicable nanoparticles in several fields is copper nanoparticles (CuNPs). CuNPs synthesis is relatively low cost and the applications such as catalytical, optical, electrical and antifungal/antibacterial show outstanding results [3].

Physical, thermal, and chemical reduction methods of nanoparticle synthesis have been widely reported. These methods are sophisticated, quite expensive, and possibly toxic [4]. Green synthesis nanoparticle using plant extracts offers an alternative approach to resolve these problems. It was a simple, environment friendly, and economical green synthesis procedure. The extract of plants was very cheap and stable against harsh environmental conditions [5].

Plant extracts are involved in redox reactions, which reduce metal ions to form nanoparticles. Metabolites such as sugar, terpenoids, polyphenols, alkaloids, phenolic acids, and proteins play essential roles in the reduction of metal ions to nanoparticles and support the stability of nanoparticles [2, 6]. Many works suggest that plant extracts such as *Solanum Lycopersicum* [7], *Eclipta prostrate* [3], *Punica granatum* [8], *Plantago asiatica* [9], *Gnidia glauca* and *Plumbago zeylanica* [10], *Uncaria gambir* Roxb [11], *Camellia sinensis* [12], *Moringa oleifera* [13], *Crataegus pontica* L [14], dates [15] and other plants have been explored for CuNPs synthesis. Different plants produce different nanoparticle characteristics.

Our study used *Piper retrofractum* Vahl fruit extracts for the synthesis of CuNPs. *Piper retrofractum* Vahl, a member of family *Piperaceae*, also known as Java chili in Indonesia, has been reported as antioxidant [16], mosquito larvacide [17, 18], anti-pest [19], antimicrobial [20, 21], insecticide [22], anti-dengue virus [23], antiobesity [24], cytotoxic/anticancer [25, 26, 27], antifungal [25] and antituberculosis [28].

* Corresponding author.
E-mail addresses: sabarjpn@ub.ac.id, sabarjpn@gmail.com (A. Sabarudin).

https://doi.org/10.1016/j.heliyon.2020.e04636
Received 3 March 2020; Received in revised form 13 July 2020; Accepted 3 August 2020

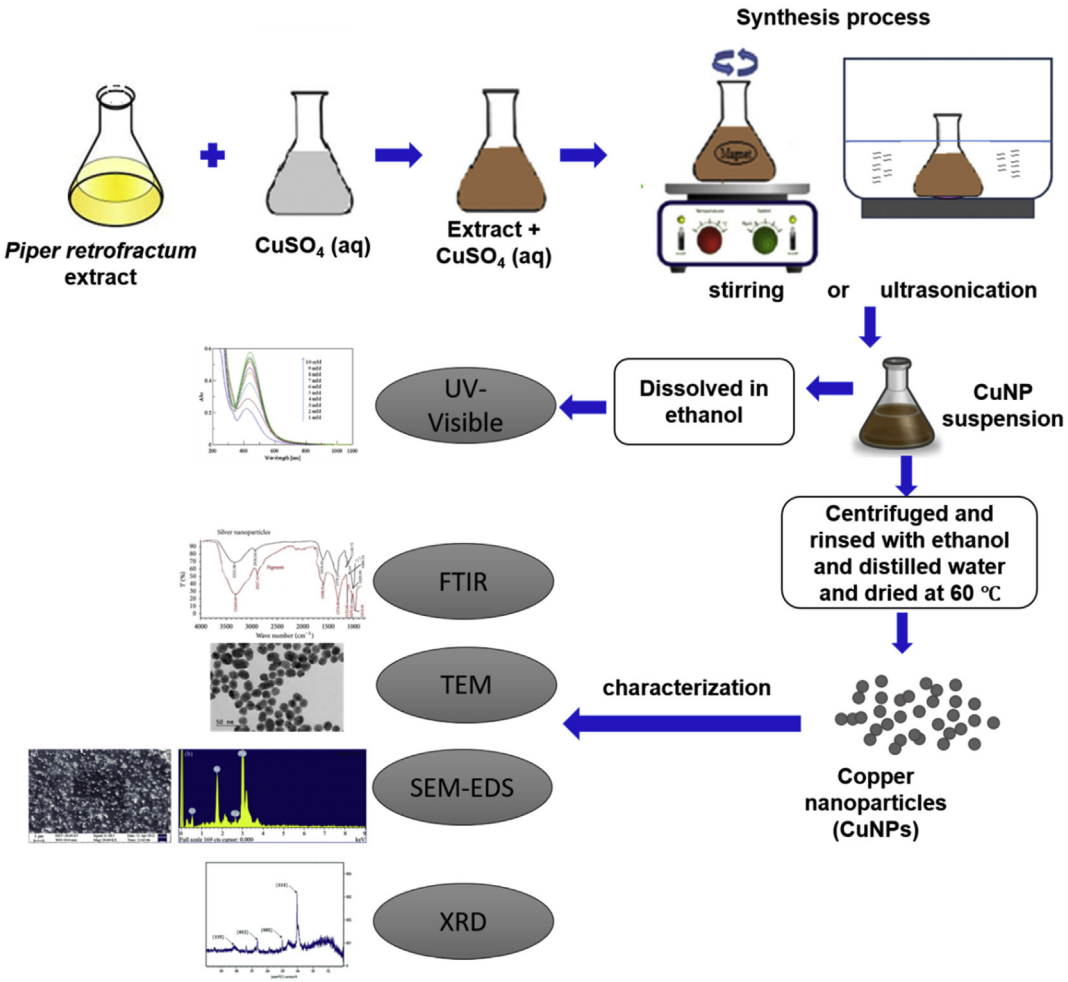

Figure 1. Scheme of green synthesis process and characterization of CuNPs.

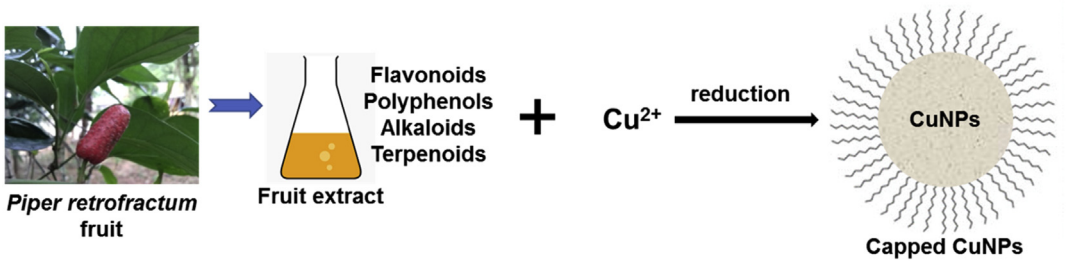

Figure 2. Illustration picture for the CuNPs formation using *Piper retrofractum* fruit extract.

However, it has never been reported as a natural reagent for the green synthesis of nanoparticles.

The phytochemical test of *Piper retrofractum* extract shows the presence of flavonoid, alkaloid, tannin, and steroid/terpenoid compound groups [28]. In addition, several studies have shown that the primary and secondary metabolite compounds in *Piper retrofractum* include piperidine alkaloids [24], phenylpropanoids [29], and amides [25]. So far, the previous study had shown 33 compounds successfully isolated from this plant [25]. These compounds have potential as reducing as well as capping/stabilizing agents for the synthesis of nanoparticles [30, 31]. Accordingly, in this work, we reported for the first time the use of medicinal plant *Piper retrofractum* Vahl fruit extracts to synthesize CuNPs. Some parameters, which include extract concentration of the plant, pH, temperature, and reaction time, were investigated. The properties of CuNPs were then characterized using UV-vis, FTIR, XRD, SEM-EDS, and TEM. The synthesized CuNPs in this work showed the spherical shape with high uniformity of the particle sizes, relatively good stability in a particular solvent, and antibacterial activity properties.

2. Materials and methods

2.1. Reagent and materials

Copper sulfate pentahydrate purchased from Sigma Aldrich (Singapore) was used as a starting material. Galic acid and Folin & Ciocalteu's phenol reagents for the determination of the total phenolic content in the extract were provided by Sigma Aldrich (Singapore). *Piper retrofractum Vahl* fruits were collected from Sumenep located in Madura

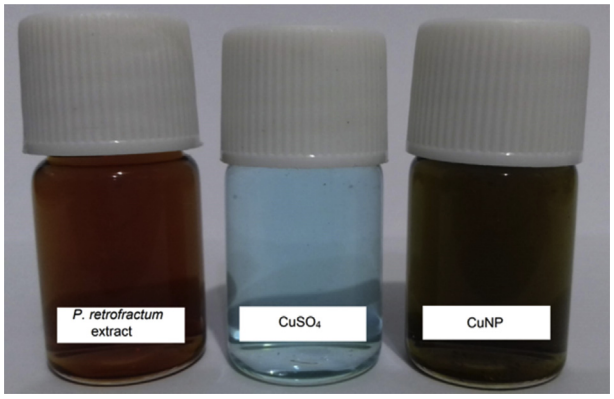

Figure 3. The color change in green synthesis of CuNPs.

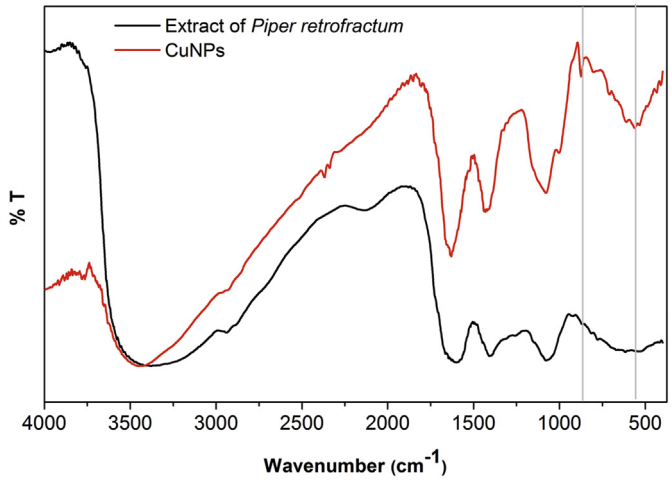

Figure 4. FTIR spectrum comparison of *Piper retrofractum* extract with CuNPs. Conditions for CuNPs preparation are extract concentration of 100%, the temperature of 60 °C, pH 4, and the reaction time of 60 min.

island, East Java, Indonesia. Distilled water was used throughout the experiment to dissolve reagents.

2.2. Preparation of Piper retrofractum Vahl. fruit extract

Piper retrofractum fruits were rinsed with running water to remove dust. Fruits were dried for 5 days at 50 °C temperature in an oven [17]. The dried fruits were ground to form a powder. The 500 mL beaker glass containing 100 g of fruit powder with 500 mL water was stirred and heated at 60 °C for 30 min. Obtained fruit broth was filtered by fabric and centrifuged at 2500 rpm for 15 min. The filtrate called extract was separated and stored at 4 °C for further use.

Table 1. FT-IR characteristic peaks of *Piper retrofractum* extract and CuNPs.

Wavenumber (cm^{-1})*		Assignment
Extract	CuNPs	
-	561.25	Cu–O
-	873.69	Cu–O–H
1078	1078.13	C–O stretching
1398.30	1431.08	C–H bending
1627.81	1635.52	O–H bending
2928.50	2900	C–H stretching
3284.55	3431.13	O–H stretching

* These wavenumbers were obtained from Figure 4.

2.3. Qualitative and quantitative analysis of phenolic content of Piper retrofractum extract

The presence of phenol in *Piper retrofractum* extract was tested with $FeCl_3$. About 0.05 g of extract was added with 1 % $FeCl_3$ solution. The presence of phenol compounds was indicated by the color change of extract to blackish green.

The extract's total phenolic content was determined by the Folin–Ciocalteu method as modified from Siddiqui et.al [32]. Briefly, 0.2 mL of crude extract (1 mg/mL) were made up to 20 mL with distilled water, mixed thoroughly with 1 mL of the Folin–Ciocalteu reagent until homogeneous and was allowed to stand for 8 min, then was followed by adding 3 mL of 10% (w/v) sodium carbonate. The mixture was allowed to stand for 2 h, and absorbance was measured at 765 nm. Separately, the same procedure was used to make the calibration curve. The calibration curve was plotted by mixing 0.2 mL aliquots of 100, 125, 150, 175, 200 μg/mL Gallic acid solutions (10-fold dilution) with 1 mL of the Folin–Ciocalteu reagent and 3 mL of 10% (w/v) sodium carbonate. The total phenolic content was calculated from the calibration curve, and the results were expressed as mg of gallic acid equivalent per gram dry weight.

2.4. Green synthesis and characterization of CuNPs using Piper retrofractum Vahl extract

The copper nanoparticle synthesis process was conducted in two methods by stirring (CORNING PC-620D) and sonication using a sonicator (DELTA Ultrasonic Cleaner DC150 DC150H). The scheme of the synthesis process was illustrated in Figure 1. An aqueous solution of copper sulfate was used as a copper ion source. In a 100 mL Erlenmeyer, 25 mL of $CuSO_4$ solution 0.1 M was mixed with 50 mL of *Piper retrofractum* extract. The effect of extract concentration was determined by varying *Piper retrofractum* extract concentrations (20, 40, 60, 80, and 100 %), and the reaction was carried out at 60 °C for 60 min. Extract concentration of 100 % was used to further reactions. To study the effect of temperature on CuNPs synthesis, the reaction mixtures were carried out at 25, 35, 60 and 80 °C for 60 min. The pH effect was studied by varying the pH of the reaction mixture (pH 4, 6, 8, and 10) and the reaction was carried out at 60 °C. The changes of pH were controlled with NaOH/HCl 0.1 M. The effect of reaction time was evaluated by conducting the reaction process for 15, 30, 45, and 60 min.

The CuNPs suspension was primarily characterized by UV–Visible spectroscopy (Shimadzu UV-Vis 1601 series). Ethanol was used as a reference, and the spectrums were recorded from 200 to 800 nm. The stability of CuNPs in water and ethanol was analyzed by measuring the absorption of CuNPs using UV-Vis after 1 day and 6 months of storage. For further analysis, synthesized CuNPs was separated by centrifugation and washed by ethanol and distilled water until the filtrate was clear. The CuNPs were dried at 60 °C to obtain a powder of CuNPs. CuNPs were characterized by employing a field emission scanning electron microscope (FESEM, FEI-Quanta FEG 650), transmission electron microscope (TEM), energy dispersive spectroscopy (EDS), X-ray diffraction (XRD, PANalytical Japan), and Fourier-transform infrared spectroscopy (FTIR, Shimadzu 8400S).

2.5. Antibacterial activity using Kirby-Bauer (disk diffusion) assay

The antibacterial activity of synthesized CuNPs was analyzed by following Kirby-Bauer (disk diffusion) assay in which bacteria species of *Staphylococcus aureus* ATCC 25923 and *Escherichia coli* ATCC 25922 were used as gram-positive bacteria and gram-negative bacteria, respectively. The paper disk was immersed in each sample (*Piper retrofractum* extract, CuNPs, sterilized water and gentamicin as negative and positive controls,

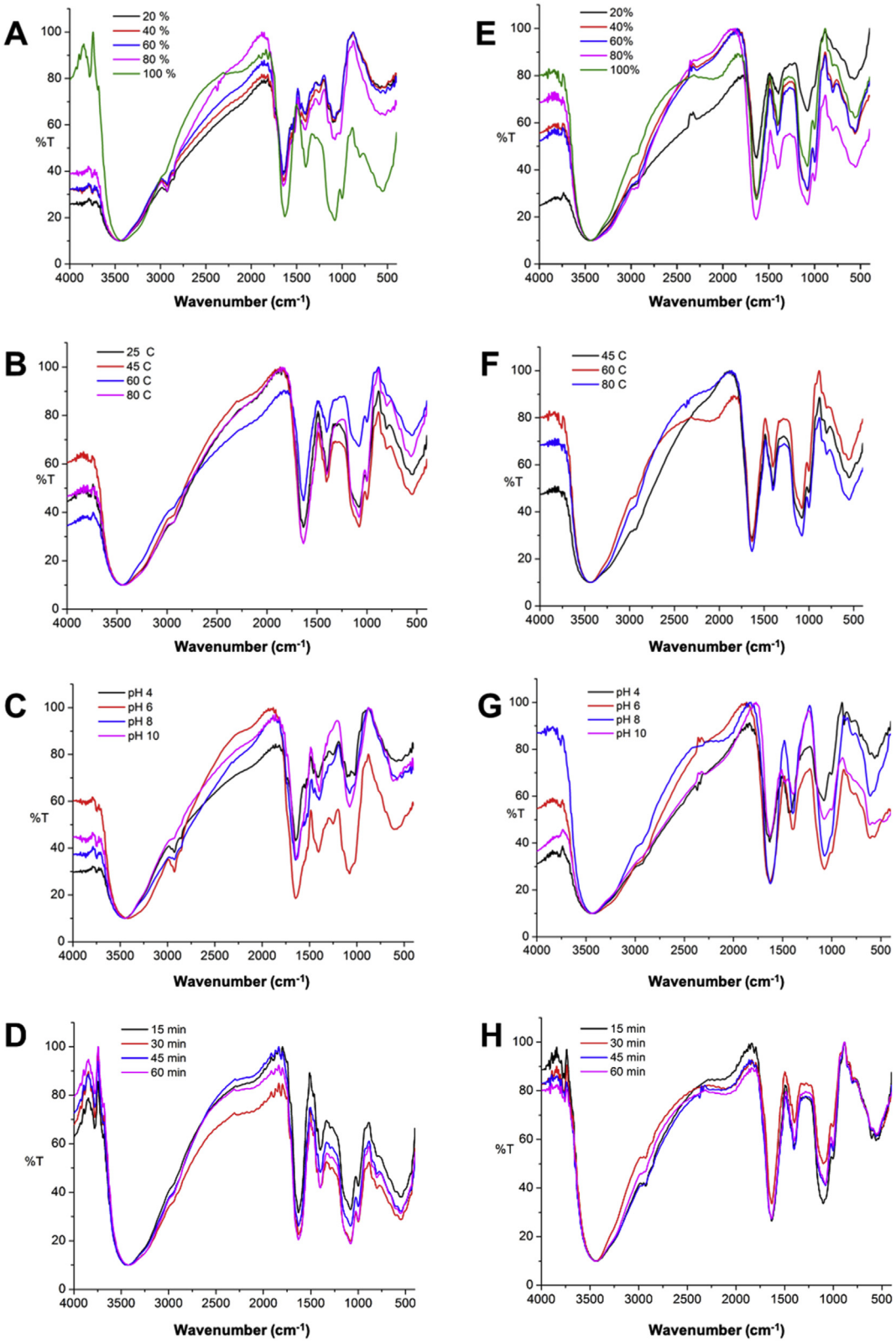

Figure 5. FTIR spectra of the synthesized CuNPs by stirring (left) and sonication (right) procedures at various extract concentrations (A–E), temperatures (B–F), pHs (C–G) and reaction times (D–H).

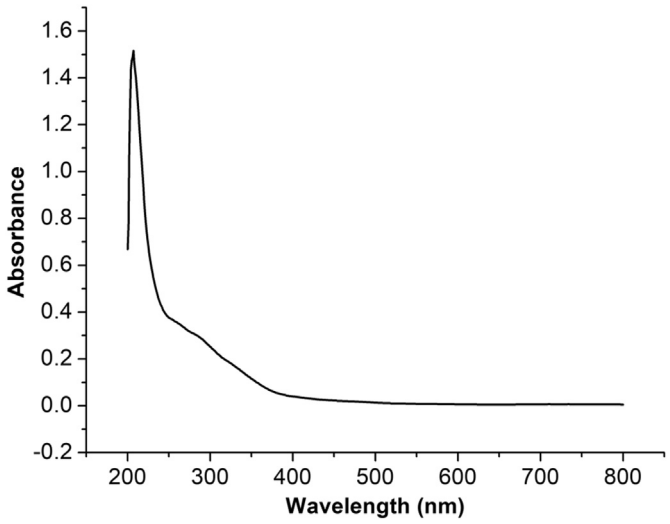

Figure 6. The UV spectrum of *Piper retrofractum* extract.

respectively) for 10 s. Then, they were placed into bacteria in the petri dish and incubated at 37 °C for 2 x 24 h. The bacterial inhibition was measured through the inhibition zone (clear zone) around the paper disk [33].

3. Results and discussion

3.1. Synthesis and mechanism of CuNPs formation

Although various metallic nanoparticles have been synthesized by employing biological materials such as plants, bacterial, fungi, and algae as natural reagents, however, the exact mechanism of the synthesis process remains challenges, thus providing opportunities for further study. For example, when nanoparticles are synthesized using a plant extract, all compounds contained in an extract are used directly without isolating a particular compound. These compounds play their roles not only as reducing agents but also as capping agents in complex systems (crude extract). If we isolate an only particular compound from an extract, it may produce nanoparticles with size, shape, uniformity, and application (i.e, antibacterial agent) that probably not be as good as using a whole extract. Of course, the basic principle of the synthesis of CuNPs in this work is the reduction of copper ions by compounds containing in *Piper retrofractum* fruit extracts followed by capping the resulted nanoparticles by compounds in the same extract.

The formation of CuNPs in this work is likely to occur through the reduction of copper ions by flavonoids or phenolic acids existing in *Piper retrofractum* extracts through the following steps (1) complexation with Cu ions, (2) simultaneous reduction of Cu ions into Cu, and (3) capping the nanoparticles with oxidized polyphenol. In this work, *Piper retrofractum* extract contained phenolic compounds as evidenced by blackish color changes using the $FeCl_3$ test. Phenolic compounds have redox properties so they can act as bio-reducing agents in the formation of nanoparticles. The –OH groups present in flavonoids are responsible for the reduction of nanoparticles. It has been proposed that hydrogen ions are released during the tautomeric transformation of the enol form of flavonoids to keto form, resulting in the reduction of metal ions and formation of metal nanoparticles [34]. In this study, the total phenolic content of *Piper retrofractum* extract was approximately about 0.98 mg GAE/g. *Piper retrofractum* extracts also contain piperidine alkaloids [24], phenylpropanoids [29], and amides [25] that can act as capping agents in the formation of CuNPs. The illustration picture for the formation of CuNPs using *Piper retrofractum* fruit extract is given in Figure 2.

The synthesized CuNPs were confirmed by the visible color change of $CuSO_4$ solution from pale blue to dark green, indicating CuNPs formation as shown in Figure 3.

FTIR and UV analyses were used to identify the formation of CuNPs. The role of *Piper retrofractum* extracts and the corresponding functional groups towards synthesis and stabilization of CuNPs were studied by recording the FT-IR spectra of the extract before and after synthesis of CuNPs (Figure 4). FT-IR spectroscopy was used to determine the functional groups of active components based on the peak value in the region of 500–4000 cm^{-1}.

As shown in Figure 4 and Table 1, FTIR spectra showed new peaks absorption of Cu–O and Cu–O–H as the additional bands compared to the extract itself, indicating the formation of CuNPs. FTIR characteristic peaks of metal-oxygen (Cu–O) were confirmed in the range 550–570 cm^{-1}, and Cu–O–H bonds led to bending absorptions in the region 870-880 cm^{-1} in all samples of the synthesized CuNPs as given in Figure 5. These results revealed the robustness of CuNPs synthesis in this work because the nanoparticles can be obtained at broad range conditions. Several peaks showed no significant changes in the region 2900 cm^{-1} (C–H stretching), 3000-3500 cm^{-1} (O–H stretching), 1600-1700 cm^{-1} (O–H bending), and 1078 cm^{-1} (C–O stretching) (Table 1). These peaks were related to functional groups inside extract compounds acting capping agents in the formation of CuNPs. This result similar to the study reported by Duman et al. [35] in which the absorption of OH group comes from functional groups existing on the surface of nanoparticles originating from the extract.

Plant extract showed a UV spectrum due to the $\pi \rightarrow \pi^*$ transition localized within the ring of the cinnamoyl and benzoyl system. Generally, this transition, which related to double bounds, was specific to flavones nuclei of extract compounds [36, 37]. The UV spectrum of *Piper retrofractum* extract (Figure 6) showed peak maxima at 207 nm, indicating the $\pi \rightarrow \pi^*$ transition of the existing polyphenolic compounds.

The UV-Vis spectrum had a similar pattern of the peak which was observed in all cases of various reaction conditions both in stirring and sonication processes. Two peaks absorption was observed at 203–210 nm (1^{st} peak) and 234–255nm (2^{nd} peak) (Figure 7). The second peak was predicted as the Surface Plasmon Resonance (SPR), demonstrating the presence of CuNPs. In previous studies, CuNPs showed SPR in an area around 562–573 nm [38, 39]. However, in our work, SPR was observed in the area around 234–255 nm (Table 2). It was probably due to the position of plasmon absorption peak which depends on several factors: the particle size, shape, type of solvent, etc. These factors were related to the refractive index of the nanoparticle medium. The surfaces of large particles are far enough from each other. Electrons need less energy to shift from their equilibrium positions, and consequently, the sufficient restoring force applying to electrons by the ions decreases as compared with smaller particles. The same explanation also applies to the shapes relating to the surface. Moreover, the structural changes of phytochemicals adsorbed on the nano surface also cause some variations of the SPR and λ_{max} [40].

3.2. Effect of extract concentration, temperature, pH and time reaction

Light green colors were observed at extract concentrations of 20 and 40 %, and dark green colors were obtained at extract concentrations of 60, 80, and 100 %. The SPR peak of CuNPs, both sonication and stirring procedures, became distinct with increasing the extract concentration (Figure 7A-E), and the maximum peak intensity was achieved at the extract concentration of 100 %. Nanoparticles with the larger size give an SPR peak at longer wavelength area (red shift), whereas a smaller size of nanoparticles allows an SPR at shorter wavelengths (blue shift) [41]. In both sonication and stirring procedures, the extract concentration of 100% resulted in a shorter wavelength of the SPR as compared to other

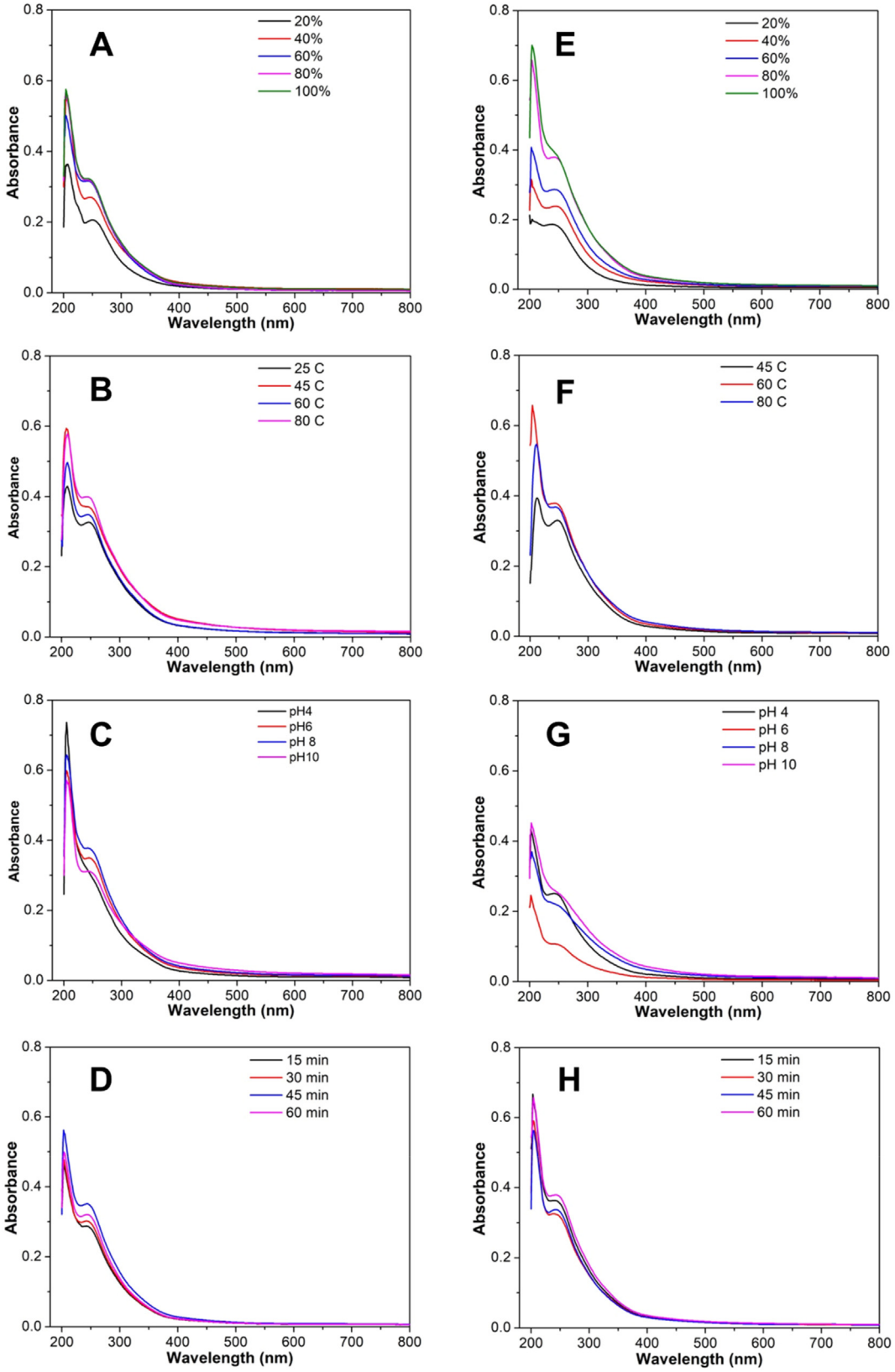

Figure 7. Comparison of UV-Visible spectra of the synthesized CuNPs by stirring (left) and sonication (right) procedures at various extract concentrations (A–E), temperatures (B–F), pHs (C–G) and reaction times (D–H).

Table 2. The wavelength (nm) of CuNPs absorptions in UV-Vis analysis.

Parameters for the formation of CuNPs		Stirring		Sonication	
		λ_1	λ_2	λ_1	λ_2
Extract concentration (%)	20	207	247.5	204	239
	40	205.5	243	203	245
	60	204	238.5	203	242
	80	203.5	234.5	204	240
	100	204	231.5	204	240
Temperature (°C)	25	210	246	-	-
	45	208	250	212	247
	60	210	243	204	240
	80	210	241	211	242
pH	4	204	246	202	249
	6	204	242.5	202	249
	8	204	240.5	204	249
	10	204.5	241	203	255
Reaction time (min)	15	203	242	203	234
	30	204	241	204	236
	45	203	242	204	240
	60	204	241	204	240

Note: λ_2 showed the presence of CuNPs.

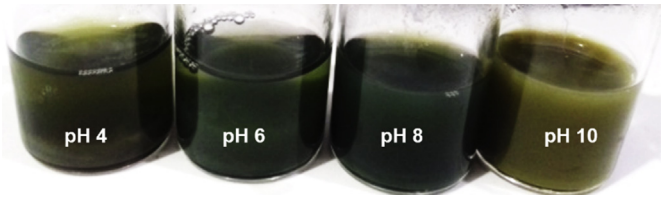

Figure 8. The changing color of the reaction mixture at various pH regions.

extract concentrations, confirming this extract produced the smallest particle sizes (Table 2).

Temperature also affected the formation of CuNPs. The highest absorbance intensity (2nd peak) was seen at the temperature of 60 °C and 80 °C for sonication and stirring processes, respectively (Figure 7B-F). At the stirring procedure, the increasing temperature showed the SPR absorption at a smaller wavelength region (Table 2), implying the formation of smaller particle sizes. In the case of sonication procedure, comparable smaller particle sizes were formed at the temperature of 60 °C (240 nm) and 80 °C (242 nm) as shown in Table 2. This condition is due to the higher temperature generates faster reactant consumption so that the resulted nanoparticles are getting smaller in size [42]. Conversely, the SPR absorption increased along with lower reaction temperatures which demonstrated the formation of larger particle sizes in both stirring and sonication procedures.

Acidity affected the colors of reaction mixture and SPR. The color of the reaction mixture turned green and the intensity got darker along with increasing pH from 2 to 6. The yellowish-green of the reaction mixture color and the precipitate were found at pH 10 (Figure 8). The SPR peak showed absorption at smaller wavelengths under alkaline condition (pH 8, by stirring procedure) and acidic to alkaline conditions (pH 4–8, by sonication procedure) as demonstrated in Figure 7C-G and Table 2. These results suggested that the smallest particle size of CuNPs is obtained at pH 8 for the stirring method, whereas a comparable size of nanoparticles was attained at wider range pH regions for the sonication procedure. Generally, acidic pH regions can cause inactivity of some biomolecules existing in the extract led to the smaller size of the produced nanoparticles. Further explanation of these results is confirmed by TEM analysis in the later section.

The color intensity of the reaction mixture increased along with the longer reaction time due to the increase in the amount of CuNPs formed. The reaction time of 15 min by sonication procedure showed the smallest particle size of the resulted CuNPs as indicated by the lowest wavelength of the SPR peak, but only a tiny amount of CuNPs was obtained. However, the stirring procedure resulted in comparable SPR peaks for all reaction times examined (15–60 min), demonstrating similar particle sizes formation (Figure 7D-H). The intensity and peak position of SPR

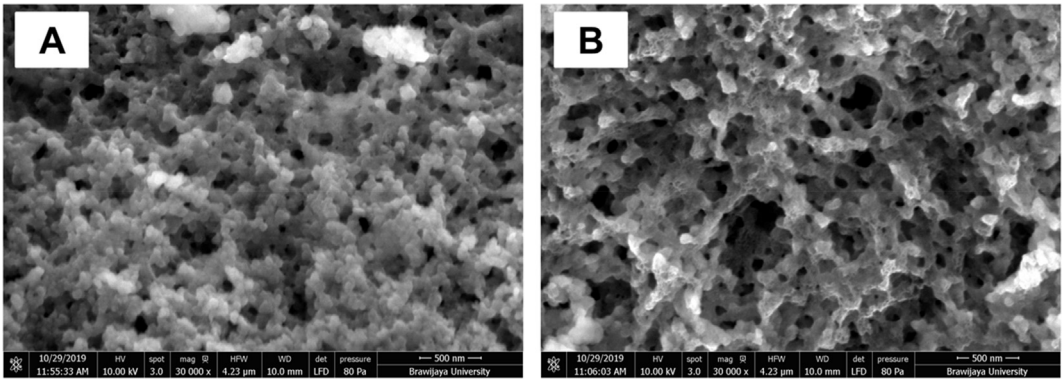

Figure 9. SEM analysis of CuNPs synthesized by stirring (A) and sonication (B) at 60 °C for 60 min without pH adjustment.

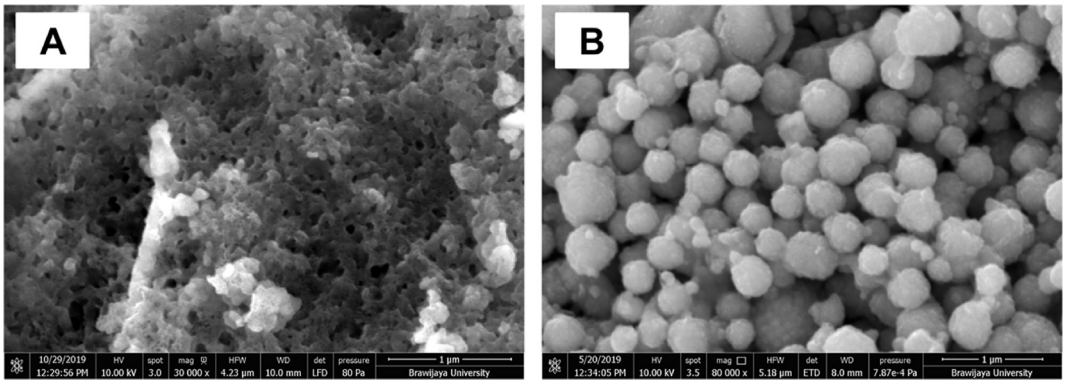

Figure 10. SEM analysis of CuNPs synthesized by sonication procedure at pH 4 (A) and pH 10 (B).

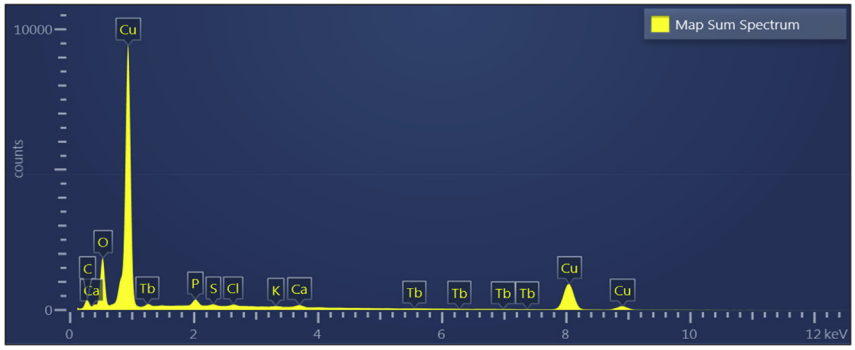

Figure 11. EDS spectrum of copper nanoparticles (CuNPs).

Table 3. Elemental composition of CuNPs by EDS analysis.

Element	Wt%
Cu	70.3
O	15.0
C	12.2
P	1.2
Ca	0.6
Cl	0.3
S	0.2
K	0.2
Tb	0.0

spectrum absorption depend on the amount and size of nanoparticles. Absorption at longer wavelengths is caused by scattering light of larger particles [38, 41]. Additionally, the type of biological material (extracts) and metal salts also influence these conditions for the synthesis of nanoparticles [43].

3.3. Characterization of CuNPs by SEM, TEM, XRD, and EDS

The morphology of CuNPs was evaluated by FESEM and TEM analysis. FESEM analysis showed that the synthesized CuNPs were spherical and tended to form a random aggregate. However, synthesized CuNPs by the sonication process was more clearly shaped (less aggregated) (Figure 9). In the reaction conditions of pH 10 with the sonication process, the CuNPs were more uniform and no aggregation, but the size was larger than pH 4 (Figure 10). This finding was consistent with the results of UV analysis.

EDS provided both qualitative and quantitative analysis of elements that might be involved in the formation of nanoparticles. From the EDS analysis, the purity of synthesized CuNPs was revealed as copper (Cu) was obtained in the highest amount as given in Figure 11. As shown in Table 3, the major elements of CuNPs were Cu (70.3%), O (15.0%), and C (12.2%), whereas other elements such as P, Ca, Cl, S, K, and Tb were in the range of 0.0–1.2%. All existing elements were derived from the extract of *Piper retrofractum* and a starting material.

TEM analysis provided information on the shape, size, and size distributions of nanoparticles. The size of synthesized CuNPs using *Piper retrofractum* extract had range 2–10 nm. The size distribution of CuNPs by stirring procedure showed more uniform than the sonication process (Figure 12). This result probably due to the high-frequency oscillation of the ultrasonic wave could disperse agglomerated nanoparticles into separate particles [44] so that the size distribution varies. The more uniform distributions and smaller nanoparticle sizes were also obtained under acidic condition (pH 4) in comparison to alkaline condition (pH 10) (Figure 13). This finding because some biomolecules in the extract of *Piper retrofractum* are probably inactive under acidic conditions, which can reduce the number of compounds that act as reducing and capping agent for the formation of nanoparticles, affecting the sizes of resulted CuNPs.

The crystallinity and crystallite size of copper nanoparticles synthesized at pH 10 was confirmed by XRD analysis as shown at Figure 14 (black line). The four distinct diffraction peaks at 2θ values were observed at 37.079°, 42.693°, 61.922° and 74.133°. These results are similar to the synthesis of CuNPs using *Eclipta prostrata* leaves extract as a natural reagent [3]. The crystallite size was calculated according to the modified Scherrer equation. The crystallite size and crystallinity of CuNPs were found around 56.8 nm and 26.4%, respectively. However, CuNPs prepared without pH adjustment or at acid condition did not show

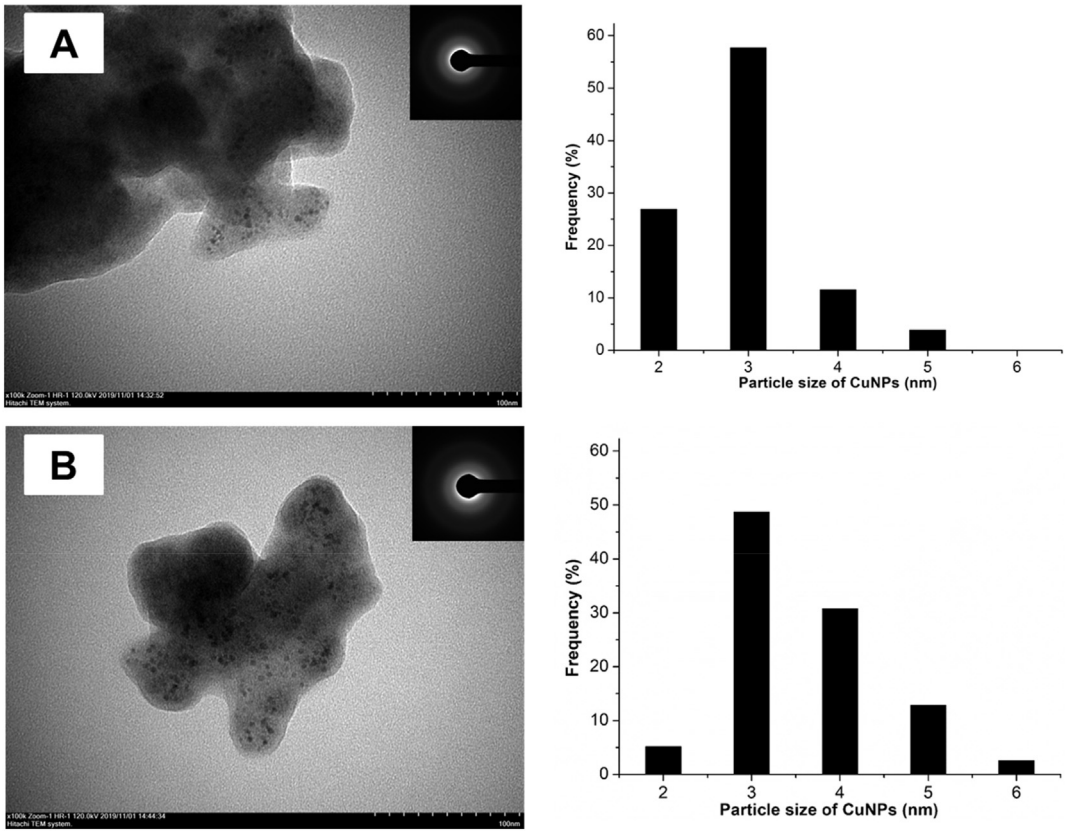

Figure 12. TEM micrograph and SAED pattern (inset), and size distribution of CuNPs synthesized by stirring (A) and sonication (B) at 60 °C for 60 min without pH adjustment.

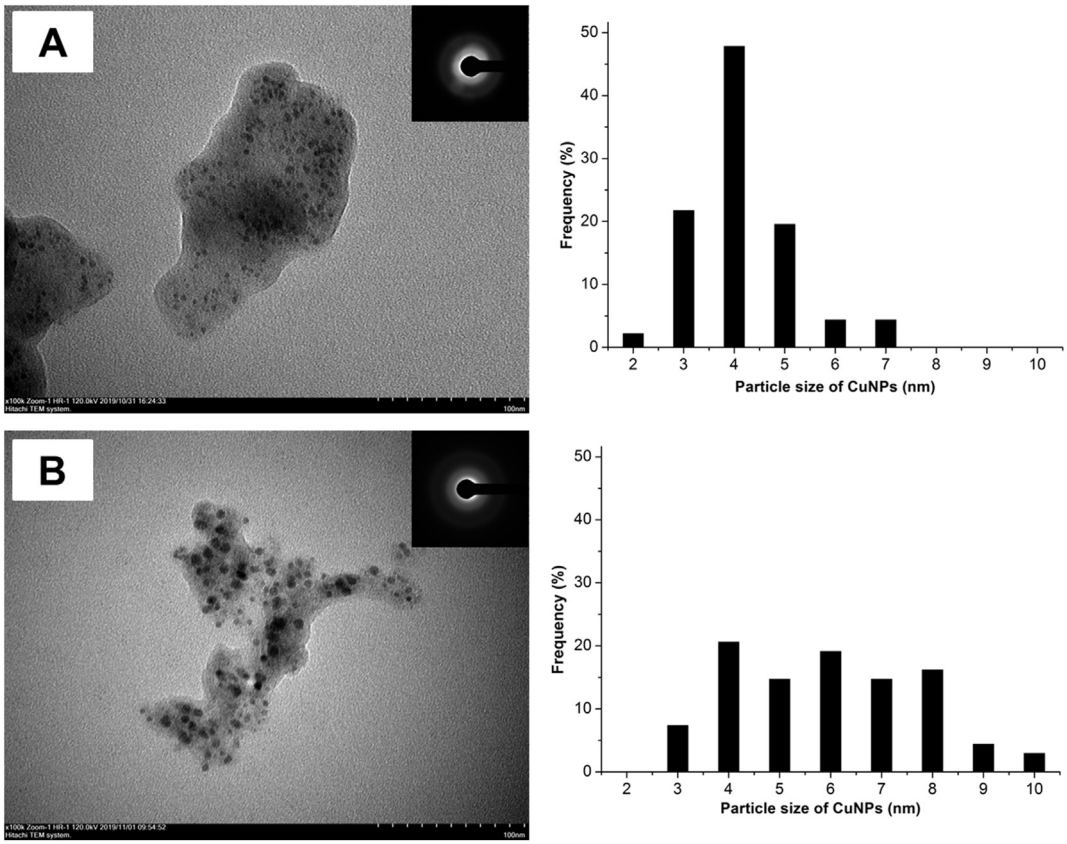

Figure 13. TEM micrograph and SAED pattern (inset), and size distribution of CuNPs synthesized by sonication at pH 4 (A) and pH 10 (B).

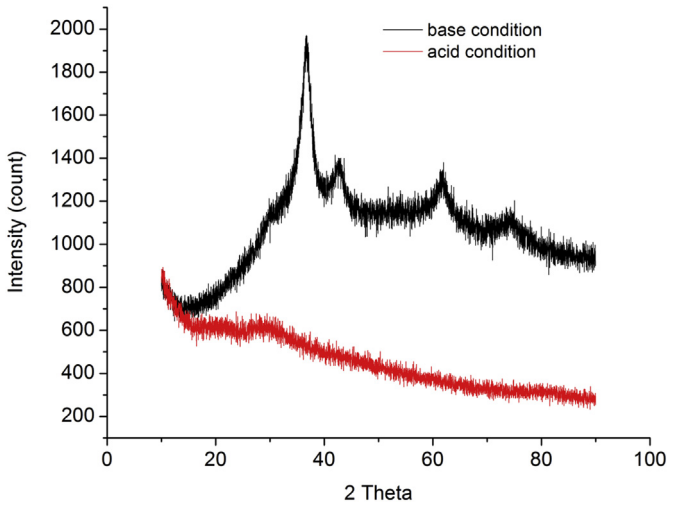

Figure 14. XRay-diffractogram of CuNPs synthesized at acid (pH 4) and base (pH 10) conditions by sonication procedure.

the crystallinity phases. These results showed good agreement with SAED pattern where the synthesized CuNPs in these conditions were predominated by the amorph phases (Figure 12 and Figure 13 A).

3.4. The stability and antibacterial activity of CuNPs

The stability of synthesized copper nanoparticle was analyzed using UV-Vis by showing the absorption peak before and after 6 months of storage of CuNPs in water and ethanol. CuNPs indicated good stability in ethanol as there is no significant change in its spectra and wavelengths as shown in Figure 15B. However, there was a slight change in the absorption spectra of CuNPs after 6 months of storage in water as shown by the existing new absorption peak (Figure 15A). This result indicated that the synthesized CuNPs are more stable in ethanol than water. Probably, this is due to the release of the capping agents from CuNPs after prolonged storage in water. Additionally, CuNPs in the biological and environmental medium (i.e., phosphate buffer saline) also showed less stability as reported by Ortelli et al. [45] and Baldisserri et al. [46].

The synthesized copper nanoparticle by sonication process was used as a sample for antibacterial activity test using disk diffusion assay, and the results were shown in Table 4 and Figure 16. The synthesized CuNPs in this work showed better antibacterial effect against *E. coli* than *S. aureus* as indicated by larger inhibition areas. This result proves that CuNPs prepared using *Piper retrofractum* extract exhibited antibacterial activity. Similar findings were also reported in which CuNPs were synthesized using tilia extract [47] and cellulosic walnut shell material [48].

The antibacterial effects of CuNPs may be associated with characteristics of membrane structure between gram-negative and gram-positive bacteria. In a previous study, *Piper retrofractum* extract alone showed antibacterial activity [20]. Our finding was in contrast with this report because the extract did not show inhibition for both *E. coli* and *S. aureus* (Table 4). This result proved that the synthesized CuNPs using this extract exhibited better inhibition of bacteria than the extract itself. A similar finding was reported for copper nanoparticles synthesized using *Pinus Merkusii Jungh & De Vriese* extract [49]. The antibacterial properties of CuNPs were related to its capability to break the bacterial cell and cause multiple toxic effects by a generation of reactive oxygen species, lipid peroxidation, protein oxidation, and DNA degradation in bacterial cell [50]. The inhibition of bacterial growth and production of reactive oxygen species were caused by electrostatic attraction between negatively charged bacterial cells and positively charged nanoparticles [51]. The CuNPs in this study possesses slightly higher antibacterial activity than the positive control (Gentamicin) as given in Table 4. Katva et al. [52] reported the collective effect of silver nanoparticles (AgNPs) with gentamicin showed better inhibition against *Enterococcus faecalis* than AgNPs alone. Probably, a combination of CuNPs with gentamicin can generate a synergistic effect that may produce a better antibacterial effect.

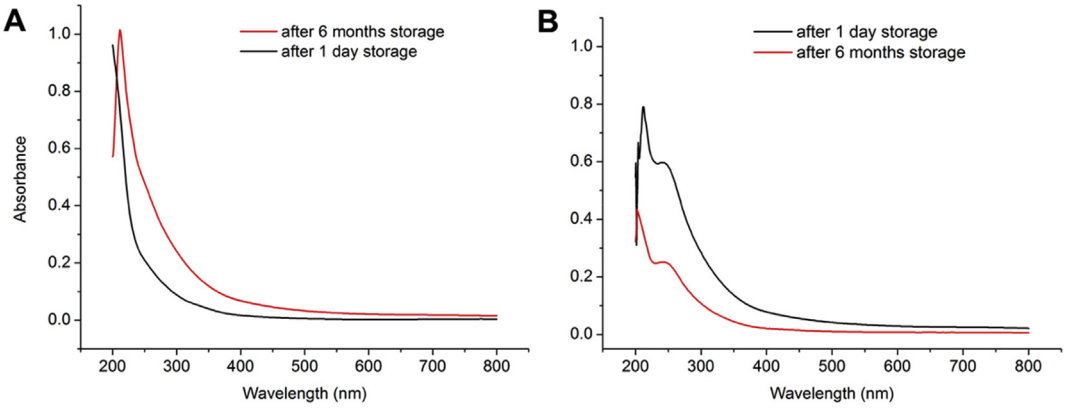

Figure 15. UV/Vis absorption spectra of CuNPs after 1 day and 6 months of storage in water (A) and ethanol (B).

Table 4. Antibacterial effect of CuNPs using disk diffusion method.

Sample	Inhibition zone (mm)	
	Staphylococcus aureus	*Escherichia coli*
CuNPs (0.2 mg/mL)	1.4	2.0
Piper retrofractum extract	0.0	0.0
Negative control (sterilized water)	0.0	0.0
Positive control (Gentamicin 0.2 mg/mL)	0.8	1.3

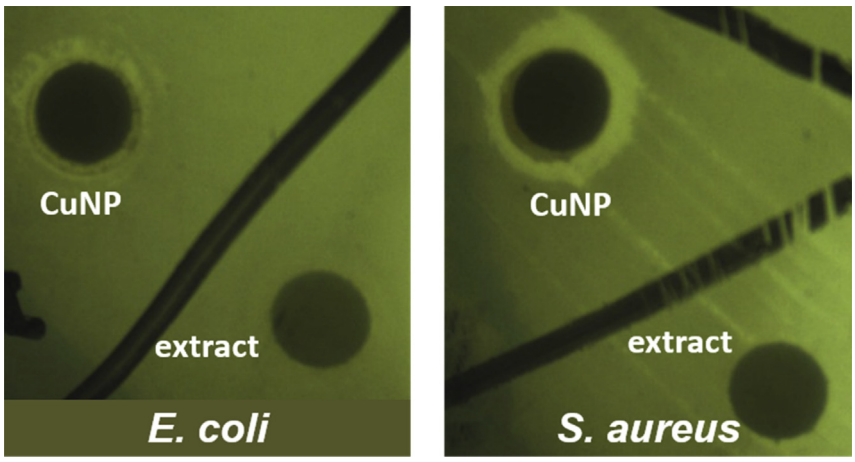

Figure 16. The comparison inhibition zone of *E. coli* with *S. aureus* exposed to CuNPs and *Piper retrofractum* extract.

4. Conclusions

The copper nanoparticles (CuNPs) were successfully synthesized by green synthesis method using *Piper retrofractum* extract. The stirring procedure produces CuNPs with a more uniform size distribution than the sonication process. Under optimized conditions, the synthesized CuNPs are spheric with the particle size of 2–10 nm, stable in certain solvent and showed antibacterial activity.

Declarations

Author contribution statement

Suci Amaliyah: Performed the experiments; Wrote the paper.

Dwika Putri Pangesti: Performed the experiments.

Masruri: Conceived and designed the experiments; Analyzed and interpreted the data; Contributed reagents, materials, analysis tools or data.

Akhmad Sabarudin: Conceived and designed the experiments; Analyzed and interpreted the data; Contributed reagents, materials, analysis tools or data; Wrote the paper.

Sutiman Bambang Sumitro: Conceived and designed the experiments; Analyzed and interpreted the data.

Funding statement

Akhmad Sabarudin was supported by Kementerian Riset Teknologi Dan Pendidikan Tinggi Republik Indonesia (Penelitian Disertasi Doktor 2019–2020 No: 167/SP2H/LT/DRPM/2019).

Competing interest statement

The authors declare no conflict of interest.

Additional information

No additional information is available for this paper.

Acknowledgements

Corresponding author (A. Sabarudin) would like to thank the Indonesian Ministry of Research and Technology/National Agency for Research and Innovation, and the Indonesian Ministry of Education and Culture, under World Class University (WCU) Program managed by Institut Teknologi Bandung for the partial support of this research.

References

[1] K. Parveen, V. Banse, L. Ledwani, Green synthesis of nanoparticles: their advantages and disadvantages, AIP Conf. Proc. 1724 (2016), 020048.
[2] M. Shah, D. Fawcett, S. Sharma, S. Tripathy, G. Poinern, Green synthesis of metallic nanoparticles via biological entities, Materials 8 (11) (2015) 7278–7308.
[3] I.-M. Chung, A.A. Rahuman, S. Marimuthu, A.V. Kirthi, K. Anbarasan, P. Padmini, G. Rajakumar, Green synthesis of copper nanoparticles using Eclipta prostrata leaves extract and their antioxidant and cytotoxic activities, Exp. Ther. Med. 14 (1) (2017) 14–18.
[4] J.I. Abd-Elkareem, H.M. Bassuony, S.M. Mohammed, H.M. Fahmy, N.R. Abd-Elkader, Eco-friendly methods of copper nanoparticles synthesis, J. Bionanoscience 10 (1) (2016) 15–37.
[5] I. Ocsoy, D. Tasdemir, S. Mazicioglu, C. Celik, A. Katı, F. Ulgen, Biomolecules incorporated metallic nanoparticles synthesis and their biomedical applications, Mater. Lett. 212 (2018) 45–50.
[6] P. Kuppusamy, M.M. Yusoff, G.P. Maniam, N. Govindan, Biosynthesis of metallic nanoparticles using plant derivatives and their new avenues in pharmacological applications – an updated report, Saudi Pharmaceut. J. 24 (4) (2016) 473–484.
[7] M. Batoool, B. Masood, Green synthesis of copper nanoparticles using Solanum Lycopersicum (tomato aqueous extract) and study characterization, J. Nanosci Nanotechnol. Res. 1 (2017) 1–5.
[8] P. Padma, S. Banu, S. Kumari, Studies on green synthesis of copper nanoparticles using Punica granatum, Annu. Res. Rev. Biol. 23 (1) (2018) 1–10.
[9] M. Nasrollahzadeh, S.M. Sajadi, M. Khalaj, Green synthesis of copper nanoparticles using aqueous extract of the leaves of Euphorbia esula L and their catalytic activity for ligand-free Ullmann-coupling reaction and reduction of 4-nitrophenol, RSC Adv. 4 (88) (2014) 47313–47318.
[10] D.A. Jamdade, D. Rajpali, K.A. Joshi, R. Kitture, A.S. Kulkarni, V.S. Shinde, J. Bellare, K.R. Babiya, S. Ghosh, Gnidia glauca - and Plumbago zeylanica -mediated synthesis of novel copper nanoparticles as promising antidiabetic agents, Adv. Pharmacol. Sci. 2019 (2019) 1–11.
[11] N. Elisma, A. Labanni, Emriadi, Y. Rilda, M. Asrofi, S. Arief, Green synthesis of copper nanoparticles using Uncaria gambir roxb. leaf extract and its characterization, Rasayan J. Chem. 12 (4) (2019) 1752–1756.
[12] A. Ahmed, M. Usman, Q.-Y. Liu, Y.-Q. Shen, B. Yu, H.-L. Cong, Plant mediated synthesis of copper nanoparticles by using Camelia sinensis leaves extract and their applications in dye degradation, Ferroelectrics 549 (1) (2019) 61–69.
[13] P.E. Das, I.A. Abu-Yousef, A.F. Majdalawieh, S. Narasimhan, P. Poltronieri, Green synthesis of encapsulated copper nanoparticles using a hydroalcoholic extract of Moringa oleifera leaves and assessment of their antioxidant and antimicrobial activities, Molecules 25 (3) (2020) 555.
[14] O. Długosz, J. Chwastowski, M. Banach, Hawthorn berries extract for the green synthesis of copper and silver nanoparticles, Chem. Pap. 74 (2020) 239–252.
[15] E.A. Mohamed, Green synthesis of copper & copper oxide nanoparticles using the extract of seedless dates, Heliyon 6 (1) (2020), e03123.
[16] N. Jadid, R.Y. Rachman, S.R. Hartanti, N. Abdulgani, W. Wikanta, W. Muslihatin, Methanol extract of Piper retrofractum vahl. potentially mediates mast cell stabilization, Int. J. Pharm. Bio. Sci. 7 (2) (2016) 379–383.
[17] U. Chansang, N.S. Zahiri, J. Bansiddhi, T. Boonruad, P. Thongsrirak, J. Mingmuang, N. Benjapong, M.S. Mulla, Mosquito larvicidal activity of aqueous extracts of long pepper (Piper retrofractum Vahl) from Thailand, J. Vector Ecol. 30 (2) (2005) 195–200.
[18] N. Komalamisra, Y. Trongtokit, K. Palakul, S. Prummongkol, Y. Samung, C. Apiwathnasorn, T. Phanpoowong, A. Asavanich, S. Leemingsawat, Insecticide susceptibility of mosquitoes invading tsunami-affected areas of Thailand, Southeast Asian J. Trop. Med. Publ. Health 37 (Suppl 3) (2006) 118–122.
[19] C. Kraikrathok, S. Ngamsaeng, V. Bullangpoti, W. Pluempanupat, O. Koul, Bio efficacy of some Piperaceae plant extracts against Plutella xylostella l. (lepidoptera: plutellidae), Commun. Agric. Appl. Biol. Sci. 78 (2) (2013) 305–309.

[20] M. Khan, M. Siddiqui, Antimicrobial activity of Piper fruits, Nat. Product. Radiance 6 (2) (2007) 111–113.
[21] W. Panphut, T. Budsabun, P. Sangsuriya, In vitro antimicrobial activity of piper retrofractum fruit extracts against microbial pathogens causing infections in human and animals, Internet J. Microbiol. 2020 (2020) 5638961.
[22] E. D. Fitriasari Dadang, D. Prijono, Effectiveness of two botanical insecticide formulations to two major cabbage insect pests on field application, J. ISSAAS. 15 (1) (2009) 42–51.
[23] N. Klawikkan, V. Nukoolkarn, N. Jirakanjanakit, S. Yoksan, C. Wiwat, K. Thirapanmethee, Effect of Thai medicinal plant extracts against dengue virus in vitro, Pharm.Sci.Asia 38 (2011) 13–18.
[24] K.J. Kim, M.-S. Lee, K. Jo, J.-K. Hwang, Piperidine alkaloids from Piper retrofractum Vahl. protect against high-fat diet-induced obesity by regulating lipid metabolism and activating AMP-activated protein kinase, Biochem. Biophys. Res. Commun. 411 (1) (2011) 219–225.
[25] R. Muharini, Z. Liu, W. Lin, P. Proksch, New amides from the fruits of Piper retrofractum, Tetrahedron Lett. 56 (19) (2015) 2521–2525.
[26] A. Hasan, K. Suryani, A. Setiyono, J. Silip, Antiproliverative activities of Indonesian Java chili, Der Pharm. Lett. 8 (2016) 141–147.
[27] S. Sriwiriyajan, T. Ninpesh, Y. Sukpondma, T. Nasomyon, P. Graidist, Cytotoxicity screening of plants of genus piper in breast cancer cell lines, Trop. J. Pharmaceut. Res. 13 (6) (2014) 921–928.
[28] M. Das, K.K. Ratha, S. Dutta, D. Mondal, J. Hazra, Comparative pharmacognostical, phytochemical and HPLC study of some common medicinal piper species, Int. J. Res. Ayurveda Pharm. 7 (6) (2017) 19–24.
[29] B.T. T Luyen, B.H. Tai, N.P. Thao, S.Y. Yang, N.M. Cuong, Y.I. Kwon, H.D. Jang, Y.H. Kom, A new phenylpropanoid and an alkylglycoside from Piper retrofractum leaves with their antioxidant and α-glucosidase inhibitory activity, Bioorg. Med. Chem. Lett 24 (17) (2014) 4120–4124.
[30] M.S. Akhtar, J. Panwar, Y.-S. Yun, Biogenic synthesis of metallic nanoparticles by plant extracts, ACS Sustain. Chem. Eng. 1 (6) (2013) 591–602.
[31] C. Celik, D. Tasdemir, A. Demirbas, A. Kati, O.T. Gul, B. Cimene, I. Ocsoy, Formation of functional nanobiocatalysts with a novel and encouraging immobilization approach and their versatile bioanalytical applications, RSC Adv. 8 (45) (2018) 25298–25303.
[32] N. Siddiqui, A. Rauf, A. Latif, Z. Mahmood, Spectrophotometric determination of the total phenolic content, spectral and fluorescence study of the herbal Unani drug Gul-e-Zoofa (Nepeta bracteata Benth), J. Taibah Univ. Med. Sci. 12 (4) (2017) 360–363.
[33] R. Indriatie, S. Mudaliana, Masruri, Microbial resistant of building plants of Gigantochloa apus, IOP Conf. Ser. Mater. Sci. Eng. 546 (2019), 042013.
[34] S. Some, O. Bulut, K. Biswas, A. Kumar, A. Roy, I.K. Sen, A. Mandal, O.L. Franco, İ.A. İnce, K. Neog, S. Das, S. Pradhan, S. Dutta, D. Bhattacharjya, S. Saha, P.K. Das Mohapatra, A. Bhuimali, B.G. Unni, A. Kati, A.K. Mandal, M.D. Yilmaz, I. Ocsoy, Effect of feed supplementation with biosynthesized silver nanoparticles using leaf extract of Morus indica L. V1 on Bombyx mori L. (Lepidoptera: bombycidae), Sci. Rep. 9 (2019) 14839.
[35] F. Duman, I. Ocsoy, F.O. Kup, Chamomile flower extract-directed CuO nanoparticle formation for its antioxidant and DNA cleavage properties, Mater. Sci. Eng. C 60 (2016) 333–338.
[36] S.S. Momeni, M. Nasrollahzadeh, A. Rustaiyan, Green synthesis of the Cu/ZnO nanoparticles mediated by Euphorbia prolifera leaf extract and investigation of their catalytic activity, J. Colloid Interface Sci. 472 (2016) 173–179.
[37] M. Nasrollahzadeh, S.M. Sajadi, M. Maham, Tamarix gallica leaf extract mediated novel route for green synthesis of CuO nanoparticles and their application for N-arylation of nitrogen-containing heterocycles under ligand-free conditions, RSC Adv. 5 (51) (2015) 40628–40635.
[38] T.M.D. Dang, T.T.T. Le, E. Fribourg-Blanc, M.C. Dang, Synthesis and optical properties of copper nanoparticles prepared by a chemical reduction method, Adv. Nat. Sci. Nanosci. Nanotechnol. 2 (1) (2011), 015009.
[39] M. Sampath, R. Vijayan, E. Tamilarasu, A. Tamilselvan, B. Sengottuvelan, Green synthesis of novel jasmine bud-shaped copper nanoparticles, J. Nanotechnol. 2014 (2014) 1–7.
[40] M. Atarod, M. Nasrollahzadeh, S.M. Sajadi, Green synthesis of a Cu/reduced graphene oxide/Fe 3 O 4 nanocomposite using Euphorbia wallichii leaf extract and its application as a recyclable and heterogeneous catalyst for the reduction of 4-nitrophenol and rhodamine B, RSC Adv. 5 (111) (2015) 91532–91543.
[41] X. Huang, M.A. El-Sayed, Gold nanoparticles: optical properties and implementations in cancer diagnosis and photothermal therapy, J. Adv. Res. 1 (2010) 13–28.
[42] J. Park, J. Joo, S.G. Kwon, Y. Jang, T. Hyeon, Synthesis of monodisperse spherical nanocrystals, Angew. Chem. Int. Ed. 46 (25) (2007) 4630–4660.
[43] P.S. Pimprikar, S.S. Joshi, A.R. Kumar, S.S. Zinjarde, S.K. Kulkarni, Influence of biomass and gold salt concentration on nanoparticle synthesis by the tropical marine yeast Yarrowia lipolytica NCIM 3589, Colloids Surf. B Biointerfaces 74 (1) (2009) 309–316.
[44] Y. Li, H.Q. Xie, J.F. Wang, W. Yu, Study on the preparation and properties of copper nanoparticles and their nanofluids, Adv. Mater. Res. 399–401 (2011) 606–609.
[45] R. Ortelli, A.L. Costa, M. Blosi, A. Brunelli, E. Badetti, A. Bonetto, D. Hristozov, A. Marcomini, Colloidal characterization of CuO nanoparticles in biological and environmental media, Environ. Sci. Nano 4 (6) (2017) 1264–1272.
[46] C. Baldisserri, A.L. Costa, Electrochemical detection of copper ions leached from CuO nanoparticles in saline buffers and biological media using a gold wire working electrode, J. Nanopart. Res 18 (4) (2016) 96.
[47] R. Hassanien, D.Z. Husein, M.F. Al-Hakkani, Biosynthesis of copper nanoparticles using aqueous Tilia extract: antimicrobial and anticancer activities, Heliyon 4 (12) (2018), e01077.
[48] T. Mehdizadeh, A. Zamani, S.M. Abtahi Froushani, Preparation of Cu nanoparticles fixed on cellulosic walnut shell material and investigation of its antibacterial, antioxidant and anticancer effects, Heliyon 6 (3) (2020), e03528.
[49] M. Masruri, D.N. Pangestin, S.M. Ulfa, S. Riyanto, A. Srihardyastutie, Moh.F. Rahman, A potent Staphylococcus aureus growth inhibitor of A dried flower extract of Pinus Merkusii Jungh & De vriese and copper nanoparticle, IOP Conf. Ser. Mater. Sci. Eng. 299 (2018), 012072.
[50] A.K. Chatterjee, R. Chakraborty, T. Basu, Mechanism of antibacterial activity of copper nanoparticles, Nanotechnology 25 (13) (2014) 135101.
[51] A. Arumugam, C. Karthikeyan, A.S. Haja Hameed, K. Gopinath, S. Gowri, V. Karthika, Synthesis of cerium oxide nanoparticles using Gloriosa superba L. leaf extract and their structural, optical and antibacterial properties, Mater. Sci. Eng. C 49 (2015) 408–415.
[52] S. Katva, S. Das, H. Singh Moti, A. Jyoti, S. Kaushik, Antibacterial synergy of silver nanoparticles with gentamicin and chloramphenicol against Enterococcus faecalis, Phcog. Mag. 14 (Suppl 4) (2017) S828–S833.